Journal of Theoretical and Applied Information Technology
15th December 2024. Vol.102. No. 23

ISSN: 1992-8645 www.jatit.org E-ISSN: 1817-3195

STRATIFICATION OF BREAST CANCER IMAGES BY UTILIZING SPATIAL INFORMATION AND DEEP LEARNING MODEL

[1*]RATHLAVATH KALAVATHI, [2]Dr M SWAMY DAS

[1]Research Scholar, Department of Computer Science & Engineering, Osmania University, Hyderabad, India
[2]Professor & Joint Director (Informatics), Department of Computer Science & Engineering, Chaitanya Bharati Institute of Technology, Hyderabad, India
Email: [1]rathodkalavathi005@gmail.com, [2]msdas_cse@cbit.ac.in

ABSTRACT

For the purpose of health care imaging, accurate breast cancer (BC) identification and classification is a critical task because of breast cancer tissue is too complex. BC is primary reason for women death with cancer. Due to potential strongest of deep learning in extraction of dominant features. In this paper, hybrid model is proposed for automated identification and treatment of BC namely EDNet-SVM i.e. Encoder-Decoder Net with SVM i.e., Support Vector Mechanism. The deep potential characteristics are extricated from EDNet and then breast cancer classification is done using SVM. EDNet is composition of Encoder and decoder and features are derived using long short term memory (LSTM). The segmented images are constructed using histogram equalization and morphological operations and feed to the EDNet for deriving optimal features from the breast cancer images which includes local features. The proposed EDNet-SVM model shown the high accuracy of 98.44% on considered freely available dataset BreastHis dataset and 96.34% on MIAS dataset. This paper listed performance values of three kernels of SVM (linear, cubic and Gaussian). The test outcomes concluded that the proposed model is superior than the existing state of art models. .
Keywords: *Identification, Breast cancer, Support vector mechanism, long short term memory, local features.*

1. INTRODUCTION

Cancer tumours grow abnormally and invade surrounding tissues. Benign and malignant tumours exist. Benign tumours contain noncancerous cells that grow locally and don't spread. Malignant tumours contain cancerous cells that can multiply uncontrollably, spread, and invade tissues. 2021-07-29 According to a 2012-2016 survey in India, 74.3 percent of localised breast cancer patients and 70.1% of locoregional breast cancer patients received multi-modality treatment. Due to their size, shape, and location, identifying and localising cancer cells in BC images is difficult. Other breast abnormalities include mastitis, adenopathy, and granuloma [1]. Machine learning (ML) techniques are used for educational prediction [2-4], bankruptcy prediction [5-7], pattern recognition [8–11], image editing [12-14], feature reduction [15-17], fault diagnosis [18- 20],

recognition of micro expression and face[21-23], conventional processing of language[24-25], diagnosing the patients[26-28]. It's especially useful for diagnosing BC. In recent decades, many researchers have suggested hypothesis for the stratification of automated BC. Some researchers have utilized nucleus analysis to classify cells as benign or malignant. The system's efficiency and accuracy degrade because of the complexity of traditional ML methodologies like initialisation, sub division, and extraction of features. DL can mitigate conventional challenges that are related to ML. This method is great for classificationof image and localization of objects. CNNs are famous algorithms that are related with DL. The structure of 2D image input alters the architecture of CNN[29-30]. In Chinese females, it is estimated that about 19.2% of new cancer cases are related with BC. Further 12.2% of newly diagnosed cancer cases are with BC and about 9.6% death rate is with this aspect[31-32]. Yearly screening deceases the morbidity related with BC. Mammography is the best suite for the screening of breast abnormalities and it also contains certain drawbacks like exposure to X-ray, discomfort to the patients, less sensitivity in the case of denser breasts and 7-10% negative or positive biopsies[33-34]. BUS i.e., Breast Ultrasound imaging technique is a non-invasive, economical

and fast imaging tool for the identification and treatment of breast masses in China and it is utilized to differentiate malignant from beginning masses and in this screening, the diagnostics check for suspicious abnormalities in breast and they conclude malignancy depending on the indicators of the image like posterior features, orientation and shape [35-36]. The ACR (American College of Radiology) has designed and developed the report of breast image and data system (BI-RADS) to normalize the assessment of masses of breast depending on margins, shape, orientation and echo patterns and acoustic features[35]. Despite, BI-RADS furnished the standards for assessment, the identification of mass features differ in terms of inter-osberver variability, that indulge improper usage of term and various levels of exposure[38]. Past studies concluded that low values of kappa coefficient = 0.29 to moderate intra-observer aggrement within BI-RADS features and this is not enough to differentiate malignant from benign lesions[39-40].

Ting et al. [41] used a CNN to classify BC-lesions with input layer as one and hidden layers as twenty eight and output layer as one. FWDA prevented over fitting. Their method had 89.47%,90.50% and 90.71% sensitivity, accuracy, and specificity respectively. Toçar et al. [42] suggested BreastNet and it contains pooling, convolution, residual and blocks with high density. This approach accuracy is 98.80% and it has outperformed VGG-19, VGG-16 and AlexNet Abbas [43] concluded a variable multi layer architecture related to DL in order to classify benign and malignant regions of breast and it has four stages to extract the invariant features makes them into deep invariant features and to learn decision making characteristics. In [43], the MIAS dataset had 92% sensitivity, 84% specificity, 91% accuracy, and 0.91 AUC. Sha et al. [44] utilized the dataset to automatically detect and stratify BC. Their method used CNNs and grasshopper optimization and it has acquired the sensitivity, accuracy and specificity as 96%,92% and 93% respectively. Using a CNN, Charan et al. [45] detected B C and it has 6 number of CNN, 04 number of average pooling and 3 numbersof fully connected layers and utilized the function of softmax to classify the 224x224 input image. Using MIAS, this network's accuracy was 65%. Wahab et al. [46] utilized a pre-trained CNN to classify mitoses. In this they had the aspects of recall, precision and F-measure a 0.8, 0.5 and 0.621. Lotter et al conducted and furnished a model for multi classification of BC that utilizes a pre-trained network of ResNet50 and it classifies lesions a calcifications, architectural distorstion, mass, focal asymmetry or null and it has the values of sensitivity, specificity and AUC as 96.2%, 90.9% and 0.94 respectively. Jiang et al. [48] improved the categorization accuracy of BC in TL by a pre-trained network. On the BCDR-F03 dataset, GoogleNet and AlexNet approached 0.88 accuracy. Khan et al. [49] proposed a model where in the characterstics of the image of a breast are extracted by utilizing the ResNet, GNet and VGGNet and it has an accuracy of 97.525% utilizing a role model dataset. Cao et al. [50] improvised the BC categorization performance on TL by not taking network layer fine tuning (ResNet-125). They combined feature groups using random forest dissimilarity. The "ICIAR 2018" dataset improved classification accuracy to 82.9%. Deniz et al. [51] acquired an accuracy of 91.37 percent, better than five others. Celik et al. [52] acquired an accuracy of 92.38% F-score and 91.57% accuracy.

The techniques related with DL have gained its existence in CAD systems to identify the BC during these days[53-56]. As per the modalities of data, such CAD systems are classified into 5 categories and they are ultrasound, mammogram, histopathologic and magnetic resonance imaging and has acquired better results[55-63]. ME CNN acquired an accuracy and sensitivity percentages of 96.4 and 97.7 respectively on breast MRI images. MSGRAP is a channel attentive architecture and contains multi scale grid average pooling and its segments have an accuracy of 97.8% and 80.4% accuracy and sensitivity.

The contribution of this paper as follows:

1. The segmented images with morphological operations and other histogram methods as augmented images for increasing accuracy.
2. Potential features are derived wirh EDNet and used SVM is used to breast cancer image classification.
3. Combined spatial information of images with deep learning models for better accuracy.

2. SUGGESTED MODEL

The suggested model is designed using encoder-decoder network with SVM. EDNet-SVM model is contribution of this study. In EDNet, features are derived using long short term memory

(LSTM) by taking segmented images as input and derived features. The propose model is given as follows:

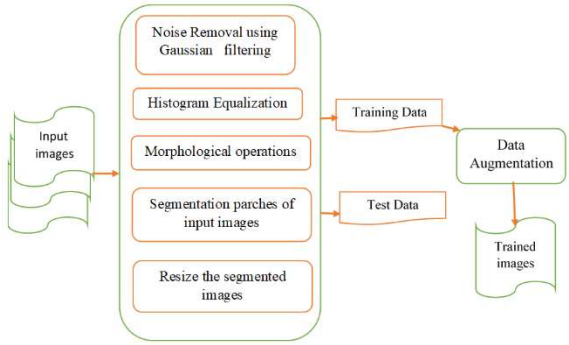

Fig. 1: Basic Architecture Of Segmentation Process.

To observe abnormalities in more accurate, pre-processing is one of the crucial step in any application. In breast cancer images, tumor regions are automatically extricated utilizing some techniques related to segmentation which results are more precise.

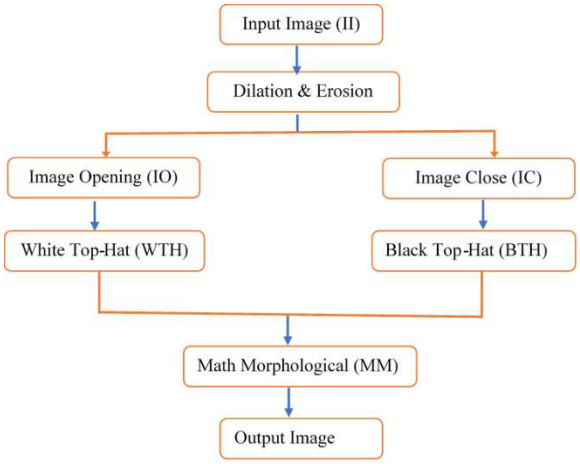

Fig.2: Morphological Operations Used In For Pre-Processing.

This work utilizes removal of noises, equalization of histogram and analyzing the morphs is done before the process of segmentation.

1. Noise removal :
   Form mammogram images, the noise will be removed using 2D mean filter of a size 3x3. Here total image is processed in 3x3 convolution (overlapped) manner and every time central pixel is replaced with mean 9 (3x3) elements.
2. Equalization of Histogram(HE):
   Equalization of Histogram is utilized to improve the image contrast. In this same intensity value is uniformly distributed in total image. By applying of the HE, abnormality is visibility is increased in mammogram.
3. Morphological operations:
   Morphological operations are used for removing non-breast regions before segmentation. In this morphological operations, structuring element (SE) is used to extract relevant structures from mammogram. The following operations are used in this work.
   Image open (IO):
   Input image is I and structuring element is SE and then open operation is defined as follows:

$$IO = (I \ominus SE) \oplus SE \quad (1)$$

   Image close (IC):
   Similarly IC can defined as follows:

$$IC = (I \oplus SE) \ominus SE \quad (2)$$

   White top-hat (WTH):
   WTH can be defined as

$$WTH = I - IO \quad (3)$$

   Black top-hat (BTH):

$$WTH = IC - I \quad (4)$$

   Mathematical Morphology (MM) :

$$MM = I + WTH - BTH \quad (5)$$

4. Segmentation
   To reduce computation time and to find exact a region which is most effected by cancer, this paper is using a threshold – based segmentation [92].
5. Resizing of image:
   The red, green and blue (RGB) breast cancer image is resized to match EDNet architecture.
6. Splitting of Data
   The total dataset is divided into training and testing in the ration of 80:20 to evaluate performance of proposed model.
7. Data augmentation

Journal of Theoretical and Applied Information Technology
15th December 2024. Vol.102. No. 23

ISSN: 1992-8645 www.jatit.org E-ISSN: 1817-3195

In deep learning models data augmentation is common step to increase the size of the dataset when the dataset size is very less. In this work, the segmented images are rotated clockwise direction and then flipped. The rotations are 90º, 180º, 270º and 360º and flipped vertically.

The segmented images of breast cancer images is given in Fig.3

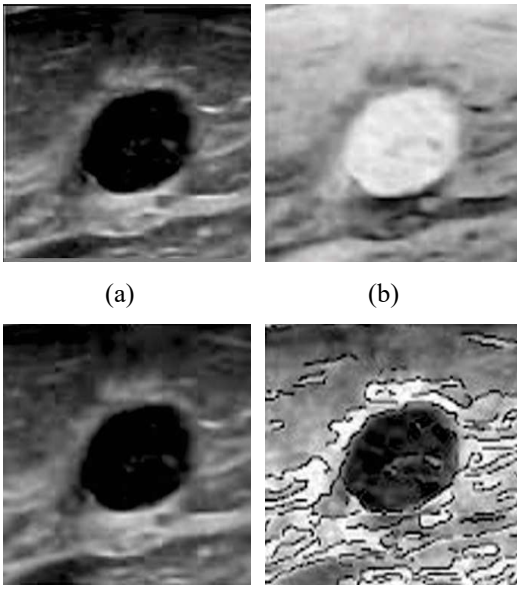

Fig.3: Ultrasound Beast Tumor Image B) Enhancement Breast Tumor Image C) ROI Shape Of Breast Tumor Image D) Segmented Breast Tumor Image.

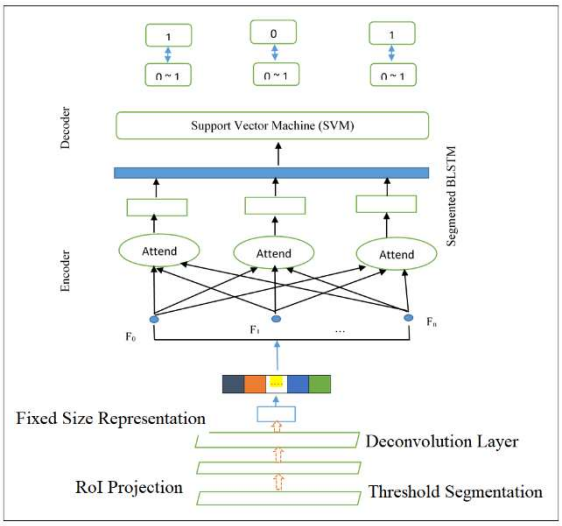

Fig.4: The Proposed Model Block Architecture.

The proposed model is given in Fig.4. This research uses EDNet (Encoder-Decoder Network) for extracting deep features. For this network, input is segmented image (Threshold based segmented image). Since the size of feature map is less, a De-convolution layer is utilized to make it bigger and help the Roi projection, that forecasts the bounding box for evey super fixal to 100 feature map and the cropped characteristics are pooled into a fixed constant size by Roi pooling layer; we then introduce a super-pixel attention mechanism. Some non-important region components may look important, while important body parts may look different and be missed. Human glancing around Fixed size representation te this by expanding each super-perception pixel's field and reducing confusion.

Here a_i output layer and it is estimated by the equation

$$a_i = \sum_{j \in M(i)} \delta_{ij} . f_j (6)$$

Where M(i) is neighbor of the i^{th} super pixel. F_j is feature vector and δ_{ij} is coefficient which is calculated using

$$\delta_{ij} = \frac{e^{Sim_{ij}}}{\sum_{j \in M(i)} e^{Sim_{ij}}}, \quad Sim_{ij} = f_i^T . M f_i (7)$$

M = fully connected layer's weight matrix

Simij = Similarity in between 2 featured vectors

Much more attention scope is given to every super pixel and is confined in its adjacent neighbors that

results in a sharp decrease in the similarity time when compared with traditional global mode.

2.1 Extraction of features using decoder

Structure of bidirectional LSTMs: the proposed bidirectional LSTMs is designed using basic LSTM. The cell structure and pre-requisites are as follows.

$$f_i = \sigma\,(W_f.h_t + U_f.y_{t-1} + b_f) \quad (8)$$

$$i_t = \sigma\,(W_i.h_t + U_i.y_{t-1} + b_i) \quad (9)$$

$$g_t = tanh\,(W_g.h_t + U_g.y_{t-1} + b_g) \quad (10)$$

$$o_t = \sigma\,(W_o.h_t + U_o.y_{t-1} + b_o) \quad (11)$$

$$c_i = f_t \circ c_{t-1} + i_t \circ g_t \quad (12)$$

$$h_t = o_t \circ \tanh\,(c_t) \quad (13)$$

Where f is forget, I is the input, o is the output and g is the gates of data processing. $\sigma$is sigmoid function , c and h is the cell and hidden state.

So as to collect the spatial data, this paper using 2- bidirectional LSTMs are used. One for segmented and another one is the skipping LSTMs. These two layers used for extracting the internal relation in different directions.

The proposed LSTM used in the decoder as first layer and its structure is formulated as follows:

$$f_i = \sigma\,(W_f.x_t + U_f.h_{t-1} + b_f) \quad (14)$$

$$i_t = \sigma\,(W_i.x_t + U_i.h_{t-1} + b_i) \quad (15)$$

$$s_t = f_{Multy}\,(\sigma\,(W_s.x_t + U_s.h_{t-1} + b_s) \quad (16)$$

$$g_t = tanh\,(W_g.x_t + U_g.h_{t-1} + b_g) \quad (17)$$

$$o_t = \sigma\,(W_o.x_t + U_o.h_{t-1} + b_o) \quad (18)$$

$$c_i = f_t \circ c_{t-1} \circ (1 - S_{t-1} + i_t \circ g_t \quad (19)$$

$$h_t = o_t \circ \tanh(c_t) \quad (20)$$

The symbols meaning is same as basic LSTM cell. Here segmented gate is introduced (st) to find image boundaries. F_{Multy} is used for classifying n human actions recognition.

Another LSTM is used to skip the states having similar features. The internal structure of this as follows:

$$f_i = \sigma\,(W_f.x_t + U_f.h_{t-1} + b_f) \quad (21)$$

$$i_t = \sigma\,(W_i.x_t + U_i.h_{t-1} + b_i) \quad (22)$$

$$p_t = f_{Multy}\,(\sigma\,(W_p.x_t + U_p.h_{t-1} + b_p) \quad (23)$$

$$g_t = tanh\,(W_g.x_t + U_g.h_{t-1} + b_g) \quad (24)$$

$$o_t = \sigma\,(W_o.x_t + U_o.h_{t-1} + b_o) \quad (25)$$

$$c_i = f_t \circ c_{t-1} \circ (1 - S_{t-1} + i_t \circ g_t \quad (26)$$

$$h_t = o_t \circ \tanh\,(c_t) \quad (27)$$

All symbols meaning is same as previous. The additionally pt is added where this is the skipping gate is utilized to check the status is updated or not.

3. RESULTS AND DISCUSSION

BreakHis termed as Breast Cancer Histopathological Image Classification contains 9109 microscope photographs of breast tumor tissue which was collected fro 82 patients with an X value of 40,100,200 and 400. 2480 and 5429 benign, malignant samples with a pixel size of 700x460, 3-channel RGB, 8-bit depth for every channel and in PNG format is taken and the database is created by collaborating with P&D Laboratory in Parana, Brazil (www.prevencaoediagnose.com.br). This particular dataset is very much useful for the researchers in order to evaluate and can be a setmark. Histologically benign answers to a lesion that doesn't meet malignancy criteria, such as cellular atypia, mitosis, basement membrane disruption, or metastasis. Benign tumours are "innocent," slow-growing, and localised. Cancer is a malignant tumour that can invade, destroy, and metastasize to cause death.

Table 1: BreakHisstatistics of images.

X	Benign	Maligant	Total
40	652	1370	1995
100	644	1437	2081
200	623	1390	2013
400	588	1232	1820
# images	2480	5429	7909

Mammographic image analysis- society (MIAS) provided this work's applied mammogram database. Every image is 1024 1024 PGM. The MIAS contains 322 images: 61 benign, 52 malignant, and 209 normal. Table 2 displays data. It includes type of tumor, class abnormalities, coordinates of the abnormality centre and circle radius. The abnormality class indulge speculated

masses, architectural distortion, circumscribed masses, ill-defined masses and asymmetry.

Brain tumor detection on picture level was performed on BreakHis and MIAS datasets to assess approach performance. The BreakHis dataset has also been classified in depth. The findings of tumor detection are compared to publically available ground truth annotation. Tables 2–10 show the suggested method's ACC and AUC from benchmark datasets. Eqs. (28-34) obtains sensitivity, specificity, ACC, PPV, AUC, FPR, FNR respectively. The complete lesions pixels show true positive and negative non-tumor pixels. FP denotes the wrong identification of healthy pixels and lesion pixels which are not identified by the furnished algorithm are furnished as FN.

TPR denotes true positive rate

$$Acc = \frac{TP+TN}{TP+TN+FP+F} (28)$$

$$AUC = \int_{\infty}^{-\infty} TPR(T)FPR(T)dT (29)$$

$$Sensitivity = \frac{TP}{TP+FN} (30)$$

$$Specificity = \frac{TN}{TN+FP} (31)$$

$$PPV = \frac{TP}{TP+FP} (32)$$

$$FPR = 1 - Specificity\ (33)$$

$$FNR = 1 - Sensitivity\ (34)$$

Since the exact stratification based on segmentation lesions and extraction of descriptors, the suggested model outperforms the older methods. This model suggests the segments the tumor in one picture and at lesion levels. The acquired shape, texture and feature intensity aids in classification. The image which is tested is named as grade 1,2 or benign and grade 3,4 or malignant and are regarded as low grade and high grade tumor respectively.

Table 2: Results of proposed model (tumor & non-tumor) of BreakHis dataset utilizing linear kernel.

Cross Validation (Folds)	ACC (%)	AUC	Sensitivity	Specificity	FNR	FPR
5	97.44	0.98	93.41	97	0.09	0.1
10	98.44	0.99	94.72	96	0.07	0.1
15	97.44	0.97	95.62	95	0.51	0.1
20	96.42	0.91	91.08	96	0.02	0.1
25	97.43	0.95	89.42	95	0.03	0.1
30	96.33	0.94	88.73	94	0.06	0.1

Table 3: Results of proposed model (tumor & non-tumor) of BreakHis dataset utilizing cubic kernel.

Cross Validation (Folds)	ACC (%)	AUC	Sensitivity	Specificity	FNR	FPR
5	96.24	0.84	92.09	94	0.09	0.15
10	97.24	0.85	94.4	95	0.09	0.13
15	96.24	0.83	93.3	93	0.07	0.14
20	95.22	0.77	89.76	94	0.07	0.16
25	96.23	0.81	88.1	93	0.06	0.12
30	95.13	0.8	87.41	92	0.06	0.15

Table 4: Results of proposed model (tumor & non-tumor) of BreakHis dataset utilizing Gaussian kernel.

Cross Validation (Folds)	ACC (%)	AUC	Sensitivity	Specificity	FNR	FPR
5	97.35	0.86	93.21	96.12	0.07	0.12
10	98.35	0.87	95.52	95.12	0.07	0.12
15	97.35	0.85	94.42	94.12	0.07	0.13
20	96.33	0.79	90.88	95.12	0.05	0.13
25	97.34	0.83	89.22	94.12	0.06	0.11
30	96.24	0.82	88.53	93.12	0.06	0.11

Table 5: Results of proposed model (tumor & non-tumor) of MIAS dataset utilizing linear kernel.

Cross Validation (Folds)	ACC (%)	AUC	Sensitivity	Specificity	FNR	FPR
5	95.34	0.82	92.52	81	0.09	0.12
10	96.34	0.83	94.83	84	0.09	0.13
15	95.34	0.81	94.73	83	0.07	0.11
20	94.32	0.75	90.19	84	0.07	0.11
25	95.33	0.79	88.53	83	0.06	0.11
30	94.23	0.78	87.84	82	0.05	0.11

Table 6: Results Of Proposed Model (Tumor & Non-Tumor) Of MIAS Dataset Utilizing Cubic Kernel.

Cross Validation (Folds)	ACC (%)	AUC	Sensitivity	Specificity	FNR	FPR
5	94.14	0.68	91.2	80	0.08	0.12
10	95.14	0.69	92.51	82	0.08	0.12
15	94.14	0.67	91.41	81	0.06	0.12
20	93.12	0.61	88.87	82	0.07	0.13
25	94.13	0.65	87.21	81	0.06	0.13
30	93.03	0.64	86.52	80	0.05	0.14

Table 7: Results Of Proposed Model (Tumor & Non-Tumor) Of MIAS Dataset Utilizing Gaussian Kernel.

Cross Validation (Folds)	ACC (%)	AUC	Sensitivity	Specificity	FNR	FPR
5	95.25	0.7	92.32	84.12	0.09	0.1
10	96.25	0.71	93.63	83.12	0.13	0.11
15	95.25	0.69	91.53	82.12	0.12	0.11
20	94.23	0.63	89.99	83.12	0.11	0.22
25	95.24	0.67	88.33	82.12	0.25	0.31
30	94.14	0.66	87.64	81.12	0.22	0.41

Three variant kernels of SVM with various validation models are deployed on the benchmark datasets for the purpose of comparison of results. On BreakHis, the proposed EDNet-SVM model obtained highest accuracy for 10 fold validation as 98.44%. Similarly the remaining performance metrics are: AUC as 0.99%, sensitivity as 95.62%, specificity as 97%, FNR as 0.51 and FPR as 0.01 for linear kernel. For cubic kernel, the proposed EDNet-SVM model obtained highest accuracy for 10 fold validation as 97.24% , similarly AUC as 0.85%, sensitivity as 94.4%, specificity as 95%, FNR as 0.09 and FPR as 0.16. For Gaussian kernel, the proposed EDNet-SVM model obtained highest accuracy for 10 fold validation as 98.35% similarly AUC as 0.87, sensitivity as 95.52% , specificity as 96.12, FNR as 0.07 and FPR as 0.13.

On MIASdataset, the proposed EDNet-SVM model obtained highest accuracy for 10 fold validation i.e. 96.34%, AUC as 0.83%, sensitivity as 94.83%, specificity as 84%, FNR as 0.09 and FPR as 0.13 for linear kernel. For cubic kernel, the proposed EDNet-SVM model obtained highest accuracy for 10 fold validation i.e. 95.14%, AUC as 0.69%, sensitivity as 92.51%, specificity as 82%, FNR as 0.08 and FPR as 0.14. For Gaussian kernel, the proposed EDNet-SVM model obtained highest accuracy for 10 fold validation i.e. 96.25%, AUC as 0.71%, sensitivity as 93.63%, specificity as 84.12%, FNR as 0.13 and FPR as 0.41. The Table 10 and Fig.10 shows the comparison in between the existing and suggested methodologies.

The Table 8, gives the accuracy values of the different models and proposed model. The state-of-art models compared are SVM, Naïve Bayesian, KNNBayesian, Decision Trees, ANN & SVM

Decision trees, Association Rules AND Neural Network, Naïve Bayesian and Ensemble Method as 97.13%, 97.23%, 70%, 95.6%, 90.41% and 89.2% respectively. The Table 8, shows the superiority of proposed model when compared to existing state-of-art models.

Table 8: The Accuracy Values Of State-Of-Art Models And Proposed Model.

Models	**Acc (%)**
SVM, Naïve Bayesian, KNN [64]	97.13%
Bayesian, Decision Trees, ANN & SVM [65]	97.23%
Decision trees [66]	70%
Association Rules AND Neural Network[67]	95.6%
Naïve Bayesian [68]	90.41%
Ensemble Method [69]	89.2%
Proposed EDNet-SVM Model	98.44

4. CONCLUSIONS

In this paper, a hybride deep learning model is proposed for breast cancer detection and classificaiton. This model helps to docters to detect and diagnosis the breast cancer. This model is constitued with EDNet and SVM. EDNet is used to derive the potential features for classification. The segmented images obtained with morphological operations and histogram equalization methods. These segmented images

are feeded to EDNet model to derive optimal features for BC classificaiton. The proposed model is applied on two datasets namely BreastHis and MIAS which are having compelx breast cancer images. On both datasets, the proposed model shown its superirity in terms of all performance metrics. The fine-tuning strategies of this work improves breast cancer classificaiton accuracy on the mentioned datasets. The propsoed model (EDNet-SVM) achieved the best accuracy,AUC , Sensitivity , Specificity , FNR and FPR compared with other models. Finally it can be concluded that integrating of morphological based segmented images with EDNet and SVM acquired good accuracy when compare with state-art- models. The highest accuracy of proposed model on BreastHis and MIAS is 98.44% and 96.34% respectively.

REFERENCES

[1] J. Zhou, L. Luo, Q. Dou, H. Chen, C. Chen, G. Li, Z. Jiang, and P. Heng, ''Weakly supervised 3D deep learning for breast cancer classification and localization of the lesions in MR images,'' J. Magn. Reson. Imag., vol. 50, no. 4, pp. 1144–1151, Oct. 2019, doi: 10.1002/jmri.26721

[2] Soomro, Bahadur & Lakhan, Ghulam Rasool & Mangi, Shah Nawaz & Shah, Dr. Naimatullah. (2020). Predicting entrepreneurial intention among business students of public sector universities of Pakistan: an application of the entrepreneurial event model. World Journal of Entrepreneurship, Management and Sustainable Development, vol. 16, no. 3, pp. 219–2301, 2020.

[3] W. Zhu, C. Ma, X. Zhao, M. Wang, A. A. Heidari, H. Chen, and C. Li, ''Evaluation of sino foreign cooperative education project using orthogonal sine cosine optimized kernel extreme learning machine,'' IEEE Access, vol. 8, pp. 61107–61123, 2020

[4] A. Lin, Q. Wu, A. A. Heidari, Y. Xu, H. Chen, W. Geng, and C. Li, ''Predicting intentions of students for master programs using a chaosinduced sine cosine-based fuzzy K-nearest neighbor classifier,'' IEEE Access, vol. 7, pp. 67235–67248, 2019

[5] Y. Zhang, R. Liu, A. A. Heidari, X. Wang, Y. Chen, M. Wang, and H. Chen, ''Towards augmented kernel extreme learning models for bankruptcy prediction: Algorithmic behavior and comprehensive analysis,'' Neurocomputing, vol. 430, pp. 185–212, Mar

[6] C. Yu, M. Chen, K. Cheng, X. Zhao, C. Ma, F. Kuang, and H. Chen, ''SGOA: Annealing-behaved grasshopper optimizer for global tasks,'' Eng. Comput., vol. 2, pp. 1–28, Jan. 2021.

[7] Z. Cai, J. Gu, J. Luo, Q. Zhang, H. Chen, Z. Pan, Y. Li, and C. Li, ''Evolving an optimal kernel extreme learning machine by using an enhanced grey wolf optimization strategy,'' Expert Syst. Appl., vol. 138, Dec. 2019, Art. no. 112814.

[8] T. Wang, L. Zhao, P. Huang, X. Zhang, and J. Xu, ''Haze concentration adaptive network for image dehazing,'' Neurocomputing, vol. 439, pp. 75–85, Jun. 2021

[9] X. Zhang, J. Wang, T. Wang, R. Jiang, J. Xu, and L. Zhao, ''Robust feature learning for adversarial defense via hierarchical feature alignment,'' Inf. Sci., vol. 560, pp. 256–270, Jun. 2021.

[10] P. Huang, L. Zhao, R. Jiang, T. Wang, and X. Zhang, ''Self-filtering image dehazing with self-supporting module,'' Neurocomputing, vol. 432, pp. 57–69, Apr. 2021

[11] T. Wang, X. Zhang, R. Jiang, L. Zhao, H. Chen, and W. Luo, ''Video deblurring via spatiotemporal pyramid network and adversarial gradient prior,'' Comput. Vis. Image Understand., vol. 203, Feb. 2021, Art. no. 103135

[12] H. Zhao, H. Guo, X. Jin, J. Shen, X. Mao, and J. Liu, ''Parallel and efficient approximate nearest patch matching for image editing applications,'' Neurocomputing, vol. 305, pp. 39–50, Aug. 2018.

[13] Y. Zhao, X. Jin, Y. Xu, H. Zhao, M. Ai, and K. Zhou, ''Parallel styleaware image cloning for artworks,'' IEEE Trans. Vis. Comput. Graphics, vol. 21, no. 2, pp. 229–240, Feb. 2015.

[14] Y. Yang, H. Zhao, L. You, R. Tu, X. Wu, and X. Jin, ''Semantic portrait

color transfer with Internet images,'' Multimedia Tools Appl., vol. 76, no. 1, pp. 523–541, Jan. 2017

[15] N. Gu, M. Fan, L. Du, and D. Ren, ''Efficient sequential feature selection based on adaptive eigenspace model,'' Neurocomputing, vol. 161, pp. 199–209, Aug. 2015

[16] P. Zhou, J. Chen, M. Fan, L. Du, Y.-D. Shen, and X. Li, ''Unsupervised feature selection for balanced clustering,'' Knowl.-Based Syst., vol. 193, Apr. 2020, Art. no. 105417.

[17] M. Fan, N. Gu, H. Qiao, and B. Zhang, ''Dimensionality reduction: An interpretation from manifold regularization perspective,'' Inf. Sci., vol. 277, pp. 694–714, Sep. 2014.

[18] S. Wang, J. Xiang, Y. Zhong, and Y. Zhou, ''Convolutional neural network-based hidden Markov models for rolling element bearing fault identification,'' Knowl.-Based Syst., vol. 144, pp. 65–76, Mar. 2018

[19] S. Wang and J. Xiang, ''A minimum entropy deconvolution-enhanced convolutional neural networks for fault diagnosis of axial piston pumps,'' Soft Comput., vol. 24, no. 4, pp. 2983–2997, Feb. 2020.

[20] Q. Gao, ''A multi-sensor fault detection strategy for axial piston pump using the Walsh transform method,'' Int. J. Distrib. Sensor Netw., vol. 14, no. 4, 2018, Art. no. 1550147718772531

[21] S.-J. Wang, H.-L. Chen, W.-J. Yan, Y.-H. Chen, and X. Fu, ''Face recognition and micro-expression recognition based on discriminant tensor subspace analysis plus extreme learning machine,'' Neural Process. Lett., vol. 39, no. 1, pp. 25–43, Feb. 2014

[22] S.-J. Wang, W.-J. Yan, T. Sun, G. Zhao, and X. Fu, ''Sparse tensor canonical correlation analysis for micro-expression recognition,'' Neurocomputing, vol. 214, pp. 218–232, Nov. 2016.

[23] Y.-J. Liu, J.-K. Zhang, W.-J. Yan, S.-J. Wang, G. Zhao, and X. Fu, ''A main directional mean optical flow feature for spontaneous microexpression recognition,'' IEEE Trans. Affect. Comput., vol. 7, no. 4, pp. 299–310, Oct. 2016

[24] D. Wang, Y. Liang, D. Xu, X. Feng, and R. Guan, ''A content-based recommender system for computer science publications,'' Knowl.-Based Syst., vol. 157, pp. 1–9, Oct. 2018.

[25] R. Guan, H. Zhang, Y. Liang, F. Giunchiglia, L. Huang, and X. Feng, ''Deep feature-based text clustering and its explanation,'' IEEE Trans. Knowl. Data Eng., early access, Oct. 6, 2020, doi: 10.1109/TKDE.2020.3028943

[26] C. Feng, Z. Zhu, Z. Cui, V. Ushakov, J. Dreher, W. Luo, R. Gu, X. Wu, and F. Krueger, ''Prediction of trust propensity from intrinsic brain morphology and functional connectome,'' Hum. Brain Mapping, vol. 42, no. 1, pp. 175–191, Jan. 2021

[27] H. Wang, X. Wu, and L. Yao, ''Identifying cortical brain directed connectivity networks from high-density EEG for emotion recognition,'' IEEE Trans. Affect. Comput., early access, Jul. 30, 2020, doi: 10.1109/TAFFC.2020.3006847

[28] H. Zhang, R. Li, X. Wen, Q. Li, and X. Wu, ''Altered time-frequency feature in default mode network of autism based on improved Hilberthuang transform,'' IEEE J. Biomed. Health Informat., vol. 25, no. 2, pp. 485–492, Feb. 2021, doi: 10.1109/JBHI.2020.2993109

[29] Q. Zhang, L. T. Yang, Z. Chen, and P. Li, ''A survey on deep learning for big data,'' Inf. Fusion, vol. 42, pp. 146–157, Jul. 2018.

[30] A. Saber, A. M. Al-Zoghby, and S. Elmougy, ''Big-data aggregating, linking, integrating and representing using semantic Web technologies,'' in Proc. Int. Conf. Adv. Mach. Learn. Technol. Appl. (AMLTA), in Advances in Intelligent Systems and Computing, 2018, pp. 331–342, doi: 10.1007/978-3-319-74690-6_33.

[31] F. Bray, J. Ferlay, I. Soerjomataram, R. L. Siegel, L. A. Torre, and A. Jemal, "Global cancer statistics 2018: Globocan estimates of incidence and mortality worldwide for 36 cancers in 185 countries," CA: a cancer journal for clinicians, vol. 68, no. 6, pp. 394–424, 2018.

[32] L. Fan, K. Strasser-Weippl, J.-J. Li, J. St Louis, D. M. Finkelstein, K.-D. Yu, W.-

Q. Chen, Z.-M. Shao, and P. E. Goss, "Breast cancer in china," The lancet oncology, vol. 15, no. 7, pp. e279–e289, 2014.

[33] T. He, M. Puppala, C. F. Ezeana, Y.-s. Huang, P.-h. Chou, X. Yu, S. Chen, L. Wang, Z. Yin, R. L. Danforth et al., "A deep learning–based decision support tool for precision risk assessment of breast cancer," JCO clinical cancer informatics, vol. 3, pp. 1–12, 2019.

[34] D. B. Kopans, "An open letter to panels that are deciding guidelines for breast cancer screening," Breast cancer research and treatment, vol. 151, no. 1, pp. 19–25, 2015

[35] M. Byra, M. Galperin, H. Ojeda-Fournier, L. Olson, M. O'Boyle, C. Comstock, and M. Andre, "Breast mass classification in sonography with transfer learning using a deep convolutional neural network and color conversion," Medical physics, vol. 46, no. 2, pp. 746–755, 2019.

[36] G. Rahbar, A. C. Sie, G. C. Hansen, J. S. Prince, M. L. Melany, H. E. Reynolds, V. P. Jackson, J. W. Sayre, and L. W. Bassett, "Benign versus malignant solid breast masses: Us differentiation," Radiology, vol. 213, no. 3, pp. 889–894, 1999

[37] A. C. of Radiology, C. J. D'Orsi et al., ACR BI-RADS Atlas: Breast Imaging Reporting and Data System; Mammography, Ultrasound, Magnetic Resonance Imaging, Follow-up and Outcome Monitoring, Data Dictionary. ACR, American College of Radiology, 2013

[38] T. He, M. Puppala, R. Ogunti, J. J. Mancuso, X. Yu, S. Chen, J. C. Chang, T. A. Patel, and S. T. Wong, "Deep learning analytics for diagnostic support of breast cancer disease management," in 2017 IEEE EMBS international conference on biomedical & health informatics (BHI). IEEE, 2017, pp. 365–368.

[39] J. H. R. do Nascimento, V. Silva, and A. C. Maciel, "Accuracy of mammographic findings in breast cancer: correlation between ri-rads classification and histologic findings," Radiol. Bras., vol. 43, no. 1, pp. 91–96, 2010.

[40] W.-q. Luo, Q.-x. Huang, X.-w. Huang, H.-t. Hu, F.-q. Zeng, and W. Wang, "Predicting breast cancer in breast imaging reporting and data system (bi-rads) ultrasound category 4 or 5 lesions: A nomogram combining radiomics and bi-rads," Scientific reports, vol. 9, no. 1, pp. 1–11, 2019.

[41] F. F. Ting, Y. J. Tan, and K. S. Sim, ''Convolutional neural network improvement for breast cancer classification,'' Expert Syst. Appl., vol. 120, pp. 103–115, Apr. 2019

[42] M. Toğaçar, K. B. Özkurt, B. Ergen, and Z. Cömert, ''BreastNet: A novel convolutional neural network model through histopathological images for the diagnosis of breast cancer,'' Phys. A, Stat. Mech. Appl., vol. 545, May 2020, Art. no. 123592, doi: 10.1016/j.physa.2019.123592.

[43] Q. Abbas, ''DeepCAD: A computer-aided diagnosis system for mammographic masses using deep invariant features,'' Computers, vol. 5, no. 4, p. 28, Oct. 2016, doi: 10.3390/computers5040028.

[44] Z. Sha, L. Hu, and B. D. Rouyendegh, ''Deep learning and optimization algorithms for automatic breast cancer detection,'' Int. J. Imag. Syst. Technol., vol. 30, no. 2, pp. 495–506, Jun. 2020, doi: 10.1002/ima.22400.

[45] S. Charan, M. J. Khan, and K. Khurshid, ''Breast cancer detection in mammograms using convolutional neural network,'' in Proc. Int. Conf. Comput., Math. Eng. Technol. (iCoMET), Mar. 2018, pp. 1–5, doi: 10.1109/icomet.2018.8346384

[46] N. Wahab, A. Khan, and Y. S. Lee, ''Transfer learning based deep CNN for segmentation and detection of mitoses in breast cancer histopathological images,'' Microscopy, vol. 68, no. 3, pp. 216–233, Jun. 2019, doi: 10.1093/jmicro/dfz002

[47] W. Lotter, A. Rahman Diab, B. Haslam, J. G. Kim, G. Grisot, E. Wu, K. Wu, J. O. Onieva, J. L. Boxerman, M. Wang, M. Bandler, G. Vijayaraghavan, and A. G. Sorensen, ''Robust breast cancer detection in mammography and digital breast tomosynthesis using annotationefficient deep learning

approach,'' 2019, arXiv:1912.11027. [Online]. Available: http://arxiv.org/abs/1912.11027

[48] F. Jiang, H. Liu, S. Yu, and Y. Xie, ''Breast mass lesion classification in mammograms by transfer learning,'' in Proc. 5th Int. Conf. Bioinf. Comput. Biol., Jan. 2017, pp. 59–62, doi: 10.1145/3035012.3035022.

[49] S. Khan, N. Islam, Z. Jan, I. U. Din, and J. J. P. C. Rodrigues, ''A novel deep learning based framework for the detection and classification of breast cancer using transfer learning,'' Pattern Recognit. Lett., vol. 125, pp. 1–6, Jul. 2019, doi: 10.1016/j.patrec.2019.03.022.

[50] H. Cao, Improve the Performance of Transfer Learning Without FineTuning Using Dissimilarity-Based Multi-View Learning for Breast Cancer Histology Images (Lecture Notes in Computer Science Image Analysis and Recognition). 2018, pp. 779–787, doi: 10.1007/978-3-319-93000- 8_88.

[51] E. Deniz, A. Şengür, Z. Kadiroğlu, Y. Guo, V. Bajaj, and Ü. Budak, ''Transfer learning based histopathologic image classification for breast cancer detection,'' Health Inf. Sci. Syst., vol. 6, no. 1, pp. 1–7, Dec. 2018, doi: 10.1007/s13755-018-0057-x.

[52] Y. Celik, M. Talo, O. Yildirim, M. Karabatak, and U. R. Acharya, ''Automated invasive ductal carcinoma detection based using deep transfer learning with whole-slide images,'' Pattern Recognit. Lett., vol. 133, pp. 232–239, May 2020, doi: 10.1016/j.patrec.2020.03.011.

[53] Q. Zhang, Y. Xiao, W. Dai, J. Suo, C. Wang, J. Shi, and H. Zheng, "Deep learning based classification of breast tumors with shear-wave elastography," Ultrasonics, vol. 72, pp. 150–157, 2016

[54] S. Han, H.-K. Kang, J.-Y. Jeong, M.-H. Park, W. Kim, W.-C. Bang, and Y.-K. Seong, "A deep learning framework for supporting the classification of breast lesions in ultrasound images," Physics in Medicine & Biology, vol. 62, no. 19, p. 7714, 2017

[55] S. Duraisamy and S. Emperumal, "Computer-aided mammogram diagnosis system using deep learning convolutional fully complex-valued relaxation neural network classifier," IET Computer Vision, vol. 11, no. 8, pp. 656–662, 2017.

[56] G. Carneiro, J. Nascimento, and A. P. Bradley, "Unregistered multiview mammogram analysis with pre-trained deep learning models," in International Conference on Medical Image Computing and Computer Assisted Intervention. Springer, 2015, pp. 652–660.

[57] R. K. Samala, H.-P. Chan, L. M. Hadjiiski, M. A. Helvie, K. H. Cha, and C. D. Richter, "Multi-task transfer learning deep convolutional neural network: application to computer-aided diagnosis of breast cancer on mammograms," Physics in Medicine & Biology, vol. 62, no. 23, p. 8894, 2017

[58] H. Lee, J. Park, and J. Y. Hwang, "Channel attention module with multi-scale grid average pooling for breast cancer segmentation in an ultrasound image," IEEE Tra

[59] M. Byra, H. Piotrzkowska-Wroblewska, K. Dobruch-Sobczak, and ´ A. Nowicki, "Combining nakagami imaging and convolutional neural network for breast lesion classification," in 2017 IEEE International Ultrasonics Symposium (IUS). IEEE, 2017, pp. 1–4

[60] Z. Gandomkar, P. C. Brennan, and C. Mello-Thoms, "Mudern: Multicategory classification of breast histopathological image using deep residual networks," Artificial intelligence in medicine, vol. 88, pp. 14– 24, 2018.

[61] Y. Feng, L. Zhang, and Z. Yi, "Breast cancer cell nuclei classification in histopathology images using deep neural networks," International journal of computer assisted radiology and surgery, vol. 13, no. 2, pp. 179–191, 2018.

[62] J.-Z. Cheng, D. Ni, Y.-H. Chou, J. Qin, C.-M. Tiu, Y.-C. Chang, C.- S. Huang, D. Shen, and C.-M. Chen, "Computer-aided diagnosis with deep learning architecture: applications to breast lesions in us images and pulmonary

nodules in ct scans," Scientific reports, vol. 6, no. 1, pp. 1–13, 2016

[63] O. Hadad, R. Bakalo, R. Ben-Ari, S. Hashoul, and G. Amit, "Classification of breast lesions using cross-modal deep learning," in 2017 IEEE 14th International Symposium on Biomedical Imaging (ISBI 2017). IEEE, 2017, pp. 109–112.

[64] H.Asri, Mousannif, Hajar, Al Moatassime, Hassan, Noël, Thomas, "Using Machine Learning Algorithms for Breast Cancer Risk Prediction and Diagnosis", Procedia Computer Science,2016, vol. 83, pp.1064-1069.

[65] K.Kourou, T.Exarchos , " Machine Learning Application in Cancer Prognosis and Diagnosis",Computational and Structural Biotechnology Journal,2014.

[66] J. Guo, M.Fung, F. Iqbal, Kuppen, R. Tollenaar,J. Lebran," Revealing Early Determinants of Occurance of Breast Cancer", Information Systems Frontiers,2017 issue 6, pp.1233-1241.

[67] Karabatak M, Ince MC," An expert system for detection of breast cancer based on association rules and neural network", Expert systems with Applications",2009 March,vol 36(2),pp.3465-3469

[68] Kharya S, Soni S.," Weighted naive bayes classifier: A predictive model for breast cancer detection", International Journal of Computer Applications. 2016 Jan,vol.133(9), pp.32-37

[69] M. R. Mohebian, H. R. Marateb, M. Mansourian, M. A. Mañanas, and F. Mokarian, "A Hybrid Computer-aided-diagnosis System for Prediction of Breast Cancer Recurrence (HPBCR) Using Optimized Ensemble Learning," Computer Structral Biotechnol.ogy,2017,vol. 15, pp. 75– 85